



Published in final edited form as:

*Glycoconj J.* 2013 August ; 30(6): 609–618. doi:10.1007/s10719-012-9459-1.

## Murine isoforms of UDP-GlcNAc 2-epimerase/ManNAc kinase: Secondary structures, expression profiles, and response to ManNAc therapy

Tal Yardeni<sup>1,2</sup>, Katherine Jacobs<sup>1</sup>, Terren K. Niethamer<sup>1</sup>, Carla Ciccone<sup>1</sup>, Yair Anikster<sup>2</sup>, Natalya Kurochkina<sup>3</sup>, William A. Gahl<sup>1</sup>, and Marjan Huizing<sup>1,\*</sup>

<sup>1</sup> Medical Genetics Branch, National Human Genome Research Institute, National Institutes of Health, Bethesda, MD 20895, USA

<sup>2</sup> Sackler Faculty of Medicine, Tel Aviv University, Tel Aviv, 69978 Israel

<sup>3</sup> The School of Theoretical Modeling, Department of Biophysics, Chevy Chase, MD 20825, USA

### Abstract

The bifunctional enzyme UDP-GlcNAc 2-epimerase/ManNAc kinase (GNE) catalyzes the first two committed steps in sialic acid synthesis. Non-allosteric *GNE* gene mutations cause the muscular disorder *GNE* myopathy (also known as hereditary inclusion body myopathy), whose exact pathology remains unknown. Increased knowledge of GNE regulation, including isoform regulation, may help elucidate the pathology of *GNE* myopathy. While eight mRNA transcripts encoding human GNE isoforms are described, we only identified two mouse *Gne* mRNA transcripts, encoding mGne1 and mGne2, homologous to human hGNE1 and hGNE2. Orthologs of the other human isoforms were not identified in mice. mGne1 appeared as the ubiquitously expressed, major mouse isoform. The mGne2 encoding transcript is differentially expressed and may act as a tissue-specific regulator of sialylation. mGne2 expression appeared significantly increased the first two days of life, possibly reflecting the high sialic acid demand during this period. Tissues of the knock-in *Gne* p.M712T mouse model had similar mGne transcript expression levels among genotypes, indicating no effect of the mutation on mRNA expression. However, upon treatment of these mice with N-acetylmannosamine (ManNAc, a Gne substrate, sialic acid precursor, and proposed therapy for *GNE* myopathy), *Gne* transcript expression, in particular *mGne2*, increased significantly, likely resulting in increased Gne enzymatic activities. This dual effect of ManNAc supplementation (increased flux through the sialic acid pathway and increased Gne activity) needs to be considered when treating *GNE* myopathy patients with ManNAc. In addition, the existence and expression of GNE isoforms needs consideration when designing other therapeutic strategies for *GNE* myopathy.

### Keywords

*GNE* myopathy; isoforms; mouse; UDP-GlcNAc 2-epimerase/ManNAc kinase

### Introduction

Uridine diphosphate (UDP)-N-acetylglucosamine (GlcNAc) 2-epimerase/N-acetylmannosamine (ManNAc) kinase (GNE), is the bifunctional key enzyme of sialic acid

\* Address correspondence to: Marjan Huizing, Ph.D. NHGRI/NIH 10 Center Drive, MSC 1851 Bld 10, Rm 10C103 Bethesda, MD 20895-1851 USA Tel.: 301-402-2797 Fax: 301-480-7825 mhuizing@mail.nih.gov.

biosynthesis, and is encoded by the *GNE* gene [1,2]. The GNE enzyme consists of 722 amino acids, encoding two enzymatic domains. The N-terminal domain (amino acid 1-378) carries out UDP-GlcNAc epimerase function, whereas the C-terminal domain (amino acids 410-722) is responsible for ManNAc kinase activity. In mammals, the end product of sialic acid synthesis, cytidine monophosphate-N-acetylneuraminic acid (CMP-Neu5Ac), feedback-inhibits GNE-epimerase activity by binding to its allosteric site (amino acids 263-266) [3,4]. Neu5Ac is the most abundant mammalian sialic acid and the precursor of most naturally existing sialic acids [5]. Sialic acids are negatively charged, terminal residues on glycoconjugates, and assist in many cellular recognition, interaction and proliferation events, both in healthy and malignant cells [5,6].

We recently demonstrated that apart from the reported 3 human GNE isoforms (GNE1-3) [7,8], five additional novel human isoforms (GNE4-8) exist and display a tissue-specific expression and different structural features with respect to catalytic activity, ligand binding and allosteric regulation [9]. However, it remains unknown which role these isoforms play in GNE regulation, or GNE-related disease pathology.

The human disorder *GNE* myopathy or Hereditary Inclusion Body Myopathy (HIBM; OMIM#600737), and its allelic Japanese disorder, Distal Myopathy with Rimmed Vacuoles (DMRV; OMIM#605820), are associated with predominantly missense mutations in *GNE*. *GNE* myopathy is autosomal recessive inherited and characterized by adult onset, slowly progressive muscle weakness and atrophy. More than 1000 *GNE* myopathy patients are estimated to exist worldwide, harboring over 80 *GNE* mutations. These mutations lead to decreased (but not absent) GNE enzymatic activities and, presumably, decreased sialic acid production [2,10,11].

To further study the pathology of *GNE* myopathy and to test possible treatment methods, mouse models of the disease were created. A complete *Gne* knockout was embryonic lethal [12]. A transgenic mouse that expressed the human *GNE* cDNA with the p.D176V mutation, common among Japanese patients, was created on a mouse background with a disrupted mouse *Gne* gene. This transgenic *Gne* p.D176V mouse model (*Gne*<sup>-/-</sup>h*GNED176V*-Tg) recapitulated the adult onset features of human *GNE* myopathy. Biochemically, the mouse presented with hyposialylation in serum and different organs [13]. A second *GNE* myopathy knock-in mouse model was created by homologous recombination through introducing the p.M712T mutation, common among Persian-Jews, into the endogenous mouse *Gne* gene. Surprisingly, these knock-in *Gne* p.M712T mouse mutants died within 72 hours of birth from severe glomerular disease. Biochemical analysis of mutant mouse kidneys revealed decreased *Gne* expression and activity as well as deficient sialylation of the major podocyte sialoproteins, podocalyxin and nephrin, suggesting that decreased production of sialic acid may be responsible for early lethality in these mice [14,15]. The mutant mice did not live long enough to study possible adult onset muscle pathology. Oral administration of the sialic acid precursor, N-acetyl-mannosamine (ManNAc), rescued the muscle phenotype in the transgenic *Gne* p.D176V mouse [16] and partially rescued the glomerular disease and early lethality in the knock-in *Gne* p.M712T mouse model [14]. The fact that human *GNE* myopathy patients have no indications of renal abnormalities, and display only a muscle phenotype, led us to further explore whether tissue- and species-specific expression of *GNE* isoforms could help explain these findings. In addition, we utilized the knock-in *Gne* p.M712T mouse model to explore effects of ManNAc supplementation on *Gne* isoform expression, which may aid in development of human clinical treatment protocols.

In mice, two different mouse *Gne* mRNA splice variants were previously described, *Gne1* and *Gne2* [17]. Here we explore the existence of other mouse *Gne* transcripts encoding additional isoforms, demonstrate differential *Gne* transcript expression in a variety of mouse

tissues, including in wild type, knock-in *Gne* p.M712T, and ManNAc supplemented mice, and perform molecular modeling studies, in an attempt to explain the differences between human and mouse *GNE* myopathy phenotypes, as well as to predict the effects of proposed *GNE* myopathy therapies on isoform expression.

## Materials and methods

### Bioinformatics

For sequence homology searches, the Protein Data Bank (pdb; <http://www.pdb.org/pdb/home/home.do>), the National Center for Biotechnology Information (NCBI) BLAST searches (<http://blast.ncbi.nlm.nih.gov/Blast.cgi>), as well as the Blat searches provided by the University of California Santa Cruz (UCSC) genome browser (<http://genome.ucsc.edu/cgi-bin/hgBlat>) were employed.

### Modeling of mGne and hGNE isoforms

Secondary structure predictions for the 31-residue N-terminal extension of the mGne2 and hGNE2 isoforms were performed by four methods: GOR V (Garnier-Osguthorpe-Robson) [18,19], FDM (Fragment Database Mining) [20], CDM (Consensus Data Mining) [21], and PSIPRED (Protein Structure Initiative Prediction) [22]. The mGne2 N-terminal extension was aligned with similar fragments of other proteins for analysis of the presence of important catalytic residues (Table 1).

### Mouse studies

Knock-in *Gne* p.M712T mice were generated as previously described [14]. All mice were maintained in the C57BL/6J background. Animals were housed in an Association for Assessment and Accreditation of Laboratory Animal Care International-accredited specific pathogen-free facility in accordance with the *Guide for the Care and Use of Laboratory Animals* (NIH publication no. 85-23). All mouse procedures were performed in accordance with protocol G04-3 approved by the Institutional Animal Care and Use Committee of the National Human Genome Research Institute. ManNAc was acquired from New Zealand Pharmaceuticals. ManNAc treatment was performed by retro-orbital injection [23] of ManNAc embedded in liposomes (ManNAc-Lipoplex) to whole litters at postnatal day 1 (P1) [24]. Untreated mice were euthanized at P1, P2, or P5. All ManNAc treated mice were euthanized at P5. All euthanasia was performed by CO<sub>2</sub> inhalation followed by cervical dislocation. For the treatment experiments we studied heterozygous (rather than wild type) tissues after ManNAc treatment, since heterozygous female mice were mated with mutant male mice, to yield a high percentage (50%) of mutants per experiment, but these did not yield any wild type pups. Heterozygous mice show no phenotype and no difference in *mGne* mRNA expression compared to wild type mice [14]. For embryonic tissue collection, pregnant mice at embryonic day 17 (E17) were euthanized, embryos were retrieved by cesarean section and euthanized by decapitation.

### RNA and cDNA

RNA was extracted from mouse tissues using the RNeasy Mini Kit (Qiagen). Tissue-specific RNA was purchased from Clontech (mouse Total RNA Master Panels). cDNA was created from all RNA using a High Capacity RNA-to-cDNA Reverse Transcription Kit (Applied Biosystems). Mouse multiple tissue cDNA panel I was purchased from Clontech (Clontech Laboratories).

## Transcript-Specific PCR

Primers were designed for transcript-specific PCR amplification of predicted mouse *Gne* splice variants (Table S1). All PCR reactions were performed with HotStarTaq polymerase, according to the manufacturer's instructions (Qiagen). PCR products were separated by agarose gel electrophoresis and selected bands were excised (QIAquick Gel Extraction Kit, Qiagen) and directly sequenced using BigDye Terminator v3.1 chemistry and an ABI 3130xl Genetic Analyzer (Applied Biosystems).

## Quantitative real-time PCR

TaqMan primers and probes were custom designed for splice variant specific sequences using the ABI Assay-by-Design service (Table S2) (Applied Biosystems). The housekeeping gene *B2M* ( $\beta 2$  microglobulin; Mm00437762) was used as internal control gene. All quantitative real-time PCR reactions and subsequent analyses were performed on an ABI PRISM 7900 HT Sequence Detection System (Applied Biosystems). The pre-run thermal cycling conditions were 10 min at 95°C to activate the *Taq* DNA-polymerase, followed by 40 cycles of 95°C for 15 s and 60°C annealing/extension for 1 min. Each experiment was performed in triplicate. Within each experiment, reactions were run in triplicate. Relative gene expression levels were determined by the comparative threshold cycle method (ddCt) [25]. For statistical analysis of the expression data, the independent samples t-test was employed (Tables S3a and S3b).

## Results

### Identification of mouse *Gne* isoform transcripts

The mouse *Gne* gene consists of 13 exons, similar to the human gene. Two mRNA transcripts exist, resulting from alternative splicing of 5' exons 1, 2 and 3, encoding 2 protein open reading frames, i.e., mGne1 (NM\_001190414) and mGne2 (NM\_015828) (Fig. 1a), as previously described [26]. Our bioinformatic database searches and PCR amplification results did not identify orthologs of the other six human isoforms (hGNE3-hGNE8) in mouse tissues.

The mGne1 protein is homologous to hGNE1 (encoded by human transcript variant 2, GenBank NM\_005476), the human isoform described in all previous biochemical and mutation analysis studies [1,2,27]; both mGne1 and hGNE1 consist of 722 amino acids with their translation start codons in exon 3, considered nucleotide 1 in this study and all previous *GNE* (mutation) reports. The mGne2 protein is homologous to human hGNE2 (encoded by human transcript variant 1, NM\_001128227), both have their translation start codons in exon 1 at nucleotide -93, yielding a 753 amino acids protein with a 31-amino acid extension at the N-terminus compared to mGne1/hGNE1 (Fig. 1).

### Modeling of mouse *Gne* isoforms

mGne1 and hGNE1 are 98.75% identical (713/722 amino acids) and 99.45% homologous (718/722 amino acids). Three of the four amino acids in mGne1 that are non-homologous to hGNE1 (E37A, S211C, and L534Q) are located in coil regions and one non-homologous amino acid, A636V, is located in an  $\alpha$ -helix. The four homologous amino acid changes between mGne1 and hGNE1 are all located in the ManNAc kinase activity encoding domain of *Gne*; N447S and L523M in an  $\alpha$ -helix domain, and R481Q and I484V in a coil domain. Our modeling analysis showed that these changes in mGne1 are not affecting secondary structure compared to hGNE1 (Fig. S1). The only amino acid change that may affect kinase enzymatic function and/or folding between hGNE and mGne is L523M. Even though the Methionine in mGne preserves the hydrophobic character of the Leucine amino acid in

hGNE, it introduces a larger side chain that may contribute to specificity of helix-helix interface interactions and may influence substrate binding and phosphorylation. The amino acid L523 in hGNE is located in the  $\alpha$ 4-helix [amino acids 516-528] of Domain I (N-lobe) of the kinase domain and is predicted to be completely immersed into the protein interior (only 5% of its area is exposed to solvent) and interacts with the  $\alpha$ 10-helix [amino acids 703-717] of the Domain II (C-lobe) of the kinase domain, which includes amino acid M712. This site is important for orientation of the two kinase subdomains (lobes) and affects GlcNAc,  $Mg^{2+}$ , and ATP binding [28,29].

mGne2 and hGNE2 are 97.08% identical (731/753 amino acids) and 98.41% homologous (741/753 amino acids). These changes include the same 8 changes mentioned above for mGne1 versus hGNE1, which are not affecting secondary structure predictions. However, the mouse mGne2 N-terminal extension of 31 amino acids is only 58.1% identical (18/31 amino acids) and 74% homologous (23/31) to that of human GNE2 (Fig. 1b). Secondary structure predictions for this extension differ significantly between mGne2 and hGNE2, in all four prediction programs (Fig. 1c). Note that secondary structure predictions of the mGne2 or hGNE2 extensions compared to themselves is very similar between prediction programs (Fig. 1c). The mGne2 N-terminal extension has similarity to some protein fragments that were also homologous to the hGNE2 extension [9], in particular with the human serum and glucocorticoid-induced kinase 1 (SGK1) and histidine (His) kinases of different organisms (Table 1). SGK1 contains an intermolecular disulfide bond [30] in the region homologous to the mGne2 and hGNE2 N-terminal extensions. In SGK1, this region is predicted to come in close contact with an activation loop of the neighboring subunit and with its phosphorylation site [30]. Interestingly, a cysteine residue is present in the N-terminal extension of hGNE2 (at residue 12), as well as in the homologous SGK1 sequence and in several homologous His kinases (Table 1). In addition, SGK1 (residues 175-240) harbors another 25% homologous region to Gne (residues 370-471 of mGne1/hGNE1). This region is located between the epimerase and kinase enzymatic domains and contains a cysteine at residue 388. The cysteine residues C12 and C388 were predicted candidates for disulfide bonds, whether intermolecular (as in SGK1) or intramolecular (possibly between GNE regions) [9]. However, mGne2 lacks this cysteine residue, and may therefore harbor different enzymatic properties, binding sites or secondary structure in its N-terminal region than hGNE2. Moreover, mGne2 has homologies to other protein fragments, which have lower homology to the hGNE2 extension, including other kinases (a Ser/Thr protein kinase and dual-specificity tyrosine phosphorylation regulated kinase 2 (DYRP2)) (Table 1), whether these homologies predict similarities in structural or binding properties is a subject of future studies.

### Tissue-specific expression of mGne1 and mGne2 encoding transcripts

Tissue-specific PCR amplification of mouse cDNA tissue panels revealed that both mouse mGne encoding transcripts were expressed in all tissues tested, except for liver which lacked mGne2 (Fig. 2).

### Expression of mGne isoforms in knock-in *Gne* p.M712T mice

For mGne transcript expression in the knock-in p.M712T mouse model, we analyzed kidney and skeletal muscle expression, because they display a *GNE* myopathy phenotype. And, additionally, liver was included because this is the only mouse tissue without mGne2 transcript expression. In kidney and skeletal muscle, there was no significant difference in mGne1 or mGne2 transcript expression between wild type (+/+) and mutant (-/-) tissues at the same age (P2 or embryonic day 17 (E17), Fig. 3a). mGne2 transcript levels were increased dramatically (significant in most cases) at P2 compared to E17 in both genotypes (Fig. 3a). Livers expressed more (significant in mutant tissues) mGne1 transcript at P2

compared to E17, similar to the mGne2 transcript increase at P2 in kidney and skeletal muscle.

Fig. 3b compares *mGne* transcript expression in tissues from mice that did not receive ManNAc (wild type only at P5, since untreated mutant mice die before P3 of severe glomerulopathy [14]) to those that received ManNAc (mutant and heterozygous). Heterozygous mice have no phenotype [14] and showed similar *mGne* transcript expression levels compared with wild type mice (Fig. 3b, tissues at P2). All untreated wild type tissues showed significantly decreased *mGne* transcript levels (both mGne1 and mGne2) at P5 compared to P2. After ManNAc treatment, *mGne* transcript levels appeared to be significantly increased in kidney and skeletal muscle, compared to untreated tissues at P5. Liver did not show this response to ManNAc treatment. There was no apparent difference in *mGne* transcript expression between genotypes after ManNAc treatment, with the exception of mGne2 transcript expression in kidney, which appeared to be slightly upregulated in mutant tissue.

## Discussion

GNE (isoform) expression and localization are important modulators of sialylation [9,31-33], and may play an important role in the pathology of *GNE* myopathy. Humans have eight GNE isoforms (hGNE1-hGNE8) [9], and mice only have two isoforms, mGne1 and mGne2 [8], with high homologies of 99.5% and 98.4% to hGNE1 and hGNE2, respectively. The *GNE* gene may be subject to evolutionary mechanisms by which the number of cellular functions can be increased, without increasing the number of genes [9,34].

mGne1, like hGNE1, is ubiquitously expressed (Fig. 2) [9] and differs from hGNE1 in only 8 amino acids, located in structurally non-important regions. Both have a similar predicted secondary structure (displayed in [9] and [29], Fig. S1). Recombinantly expressed mGne1 and hGNE1 were previously shown to both occur in the tetrameric (full enzyme activity) and dimeric (kinase activity only) states, with comparable epimerase and kinase activities [17]. These studies suggest that mGne1 and hGNE1 likely have similar biochemical functions.

mGne2 is identical to mGne1, with the exception of a novel 31-amino acids N-terminal extension (similar to hGNE2). Even though the N-terminal extensions of mGne2 and hGNE2 are encoded by homologous exons in the *Gne/GNE* genes, the amino acids of both fragments varied dramatically in composition (only 58.1% identity, Fig. 1b), secondary structure predictions (Fig. 1c), and homologies to fragments of other proteins (Table 1). mGne2 is expressed in all murine tissues tested, with the exception of liver; a pattern that is significantly different from hGNE2 expression (Fig. 2b). Recombinantly expressed mGne2 predominantly exists in the tetrameric state with full epimerase and kinase enzymatic activities, while hGNE2 predominantly exist in the dimeric state with a lack of epimerase activity [17]. The reduced homology of the mGne2 and hGNE2 N-termini apparently influences oligomer formation and the difference in epimerase activities. These results implicate that mGne2 and hGNE2 have different biochemical properties, likely due to independent evolutionary pathways.

We used our knock-in *Gne* p.M712T mouse model to further study the response of mGne isoform expression to age, sialylation status and sialylation increasing therapy. First, we demonstrated that the M712T mutation does not directly affect *Gne* mRNA expression levels. Second, we showed that mGne expression is highly responsive to age. In kidney and skeletal muscle (the two affected tissues in *Gne* p.M712T mice), mGne2 expression increased dramatically at P2 compared to E17 in all genotypes (Fig. 3a). This effect is likely

a response to the increased sialic acid demand in the first few days of life [35]. A similar increase was seen for mGne1 encoding transcripts in liver (the major organ of sialic acid synthesis, which lacks mGne2 expression), especially in mutant liver. Contrarily, at P5, mGne expression in kidney and skeletal muscle were significantly decreased compared to expression at P2 (Fig. 3b). These results agree with the decrease in sialic acid demand after the first two days of life [35]. Third, after ManNAc treatment, mGne2 transcript expression in kidney and skeletal muscle at P5 was considerably increased compared to untreated tissues at P5. Note that liver mGne1 transcripts did not show this response to ManNAc treatment. These mouse studies suggest that mGne2 transcripts are more sensitive to ManNAc treatment and sialic acid demands than mGne1 transcripts. This may be attributed to particular sensitivity of an element of the mGne2 transcript promotor to sialic acid (or ManNAc) concentration, which could be explored in future studies.

It remains greatly unknown whether monosaccharides (such as ManNAc) can directly influence gene transcription, and if so, whether they act through binding to promotor regions or whether they act as second messenger [12,31,36]. It is also intriguing to investigate CMP-sialic acid-regulated gene expression since this is produced in the nucleus [37].

Future studies may also reveal whether hGNE transcript expression in human *GNE* myopathy tissues have age-specific and treatment-specific responses similar to *GNE* myopathy mouse tissues. Tissue-specific hGNE/mGne isoform expression differences between human and mice may explain why the knock-in *Gne* p.M712T mouse develops severe glomerular disease and *GNE* myopathy patients have no indications of renal abnormalities. However, other factors may play a role as well, since humans and mice may differ in the relative importance of sialic acid to the kidney, and their protein glycosylation patterns also vary [38,39]. Of interest is that the transgenic *Gne* p.D176V mouse model, which is constructed such that it only expresses mGne1 transcripts [13], does not develop a severe kidney phenotype. This may indicate that mGne2 is not required for viability, but that mGne2 expression may 'fine-tune' or regulate (tissue-specific) sialylation.

Increased knowledge of GNE (isoform) regulation may help elucidate the pathology of *GNE* myopathy, as well as of other disorders of hyposialylation. Isoform expression needs to be considered when designing and evaluating treatment strategies, such the therapies currently under development for *GNE* myopathy patients, including ManNAc ([www.clinicaltrials.gov](http://www.clinicaltrials.gov) NCT01634750) or sialic acid (Neu5Ac) ([www.clinicaltrials.gov](http://www.clinicaltrials.gov): NCT01517880) supplementation, or *GNE* gene therapy [40,41]. Although no direct comparison between mouse (2 predicted mGne isoforms) and human GNE-isoform (8 predicted hGNE isoforms) related pathology could be made, we demonstrated that mouse *Gne* transcript expression, in particular mGne2, increased significant upon ManNAc treatment. This possibly dual effect of ManNAc supplementation (increased flux through sialic acid pathway and increased GNE activity) needs to be considered when treating *GNE* myopathy patients with ManNAc. A similar effect may occur upon sialic acid treatment. In addition, the existence and regulation of GNE isoforms needs to be considered when designing *GNE* myopathy gene therapy strategies [40,41].

## Supplementary Material

Refer to Web version on PubMed Central for supplementary material.

## Acknowledgments

We greatly appreciate the expert laboratory work of Dr. Shelley Hoogstraten-Miller, Katherine Berger, Katherine Patzel, and Adrian Astiz-Martinez. The authors thank Theresa Calhoun for her skilled assistance with mouse maintenance. We thank the HIBM Research group (Encino, CA) for providing the knock-in *Gne* p.M712T mouse

model. This work was performed in partial fulfillment of the requirements for a PhD degree of T.Y., Sackler Faculty of Medicine, Tel Aviv University, Israel. This study was supported by the Intramural Research Program of the National Human Genome Research Institute, National Institutes of Health, Bethesda, Maryland, United States (T.Y., K.J., T.K.N., C.C., W.A.G., and M.H.) and Research Funds of The School of Theoretical Modeling, Chevy Chase, Maryland, United States (N.K.).

## Abbreviations

<b>A. avenae</b>	Acidovorax avenae
<b>B2M</b>	$\beta$ 2 microglobulin
<b>BLAST</b>	Basic Local Alignment Search Tool
<b>B. subtilis</b>	Bacillus subtilis
<b>CDM</b>	Consensus Data Mining
<b>CMP</b>	Cytidine monophosphate
<b>DMRV</b>	Distal Myopathy with Rimmed Vacuoles
<b>DYRK2</b>	Dual-specificity tyrosine phosphorylation regulated kinase 2
<b>E</b>	Embryonic day
<b>E. coli</b>	Escherichia coli
<b>FDM</b>	Fragment Database Mining
<b>GCNA</b>	N-acetyl-B-D-glucosaminidase
<b>GlcNAc</b>	N-acetylglucosamine
<b>GNE</b>	UDP-GlcNAc 2-epimerase/ManNAc kinase
<b>GOR</b>	Garnier-Osguthorpe-Robson
<b>H. arsenicoxydans</b>	Herminiimonas arsenicoxydans
<b>HIBM</b>	Hereditary Inclusion Body Myopathy
<b>His</b>	Histidine
<b>H. sapiens</b>	Homo sapiens
<b>Min</b>	Minutes
<b>ManNAc</b>	N-acetylmannosamine
<b>NCBI</b>	National Center for Biotechnology Information
<b>Neu5Ac</b>	N-acetylneuraminic acid
<b>OMIM</b>	Online Mendelian Inheritance in Man
<b>P</b>	Postnatal day
<b>P. carotovorum</b>	Pectobacterium carotovorum
<b>PCR</b>	
<b>Pdb</b>	Protein databank
<b>PRPP</b>	Phosphoribosylpyrophosphate
<b>PSIPRED</b>	Protein Structure Initiative Prediction
<b>qPCR</b>	Quantitative real-time polymerase chain reaction
<b>RNA</b>	Ribonucleic acid



<b>SGK1</b>	Serum and glucocorticoid-induced kinase 1
<b>S. gordonii</b>	<i>Streptococcus gordonii</i> ;
<b>T. maritima</b>	<i>Thermotoga maritima</i>
<b>UDP</b>	Uridine diphosphate
<b>VAV1</b>	Vav-family member of guanine nucleotide exchange factors

## References

- Hinderlich S, Stasche R, Zeitler R, Reutter W. A bifunctional enzyme catalyzes the first two steps in N-acetylneuraminic acid biosynthesis of rat liver. Purification and characterization of UDP-N-acetylglucosamine 2-epimerase/N-acetylmannosamine kinase. *J. Biol. Chem.* 1997; 272:24313–24318. [PubMed: 9305887]
- Eisenberg I, Avidan N, Potikha T, Hochner H, Chen M, Olender T, Barash M, Shemesh M, Sadeh M, Grabov-Nardini G, Shmilevich I, Friedmann A, Karpati G, Bradley WG, Baumbach L, Lancet D, Asher EB, Beckmann JS, Argov Z, Mitrani-Rosenbaum S. The UDP-N-acetylglucosamine 2-epimerase/N-acetylmannosamine kinase gene is mutated in recessive hereditary inclusion body myopathy. *Nat. Genet.* 2001; 29:83–87. [PubMed: 11528398]
- Kornfeld S, Kornfeld R, Neufeld EF, O'Brien PJ. The Feedback Control of Sugar Nucleotide Biosynthesis in Liver. *Proc. Natl. Acad. Sci. U S A.* 1964; 52:371–379. [PubMed: 14206604]
- Seppala R, Lehto VP, Gahl WA. Mutations in the human UDP-N-acetylglucosamine 2-epimerase gene define the disease sialuria and the allosteric site of the enzyme. *Am. J. Hum. Genet.* 1999; 64:1563–1569. [PubMed: 10330343]
- Chen X, Varki A. Advances in the biology and chemistry of sialic acids. *ACS Chem. Biol.* 2010; 5:163–176. [PubMed: 20020717]
- Varki NM, Varki A. Diversity in cell surface sialic acid presentations: implications for biology and disease. *Lab. Invest.* 2007; 87:851–857. [PubMed: 17632542]
- Watts GD, Thorne M, Kovach MJ, Pestronk A, Kimonis VE. Clinical and genetic heterogeneity in chromosome 9p associated hereditary inclusion body myopathy: exclusion of GNE and three other candidate genes. *Neuromuscul. Disord.* 2003; 13:559–567. [PubMed: 12921793]
- Reinke SO, Hinderlich S. Prediction of three different isoforms of the human UDP-N-acetylglucosamine 2-epimerase/N-acetylmannosamine kinase. *FEBS Lett.* 2007; 581:3327–3331. [PubMed: 17597614]
- Yardeni T, Choekyi T, Jacobs K, Ciccone C, Patzel K, Anikster Y, Gahl WA, Kurochkina N, Huizing M. Identification, Tissue Distribution, and Molecular Modeling of Novel Human Isoforms of the Key Enzyme in Sialic Acid Synthesis, UDP-GlcNAc 2-Epimerase/ManNAc Kinase. *Biochemistry.* 2011; 50:8914–8925. [PubMed: 21910480]
- Huizing M, Krasnewich DM. Hereditary inclusion body myopathy: a decade of progress. *Biochim. Biophys. Acta.* 2009; 1792:881–887. [PubMed: 19596068]
- Noguchi S, Keira Y, Murayama K, Ogawa M, Fujita M, Kawahara G, Oya Y, Imazawa M, Goto Y, Hayashi YK, Nonaka I, Nishino I. Reduction of UDP-N-acetylglucosamine 2-epimerase/N-acetylmannosamine kinase activity and sialylation in distal myopathy with rimmed vacuoles. *J. Biol. Chem.* 2004; 279:11402–11407. [PubMed: 14707127]
- Schwarzkopf M, Knobloch KP, Rohde E, Hinderlich S, Wiechens N, Lucka L, Horak I, Reutter W, Horstkorte R. Sialylation is essential for early development in mice. *Proc. Natl. Acad. Sci. U S A.* 2002; 99:5267–5270. [PubMed: 11929971]
- Malicdan MC, Noguchi S, Nonaka I, Hayashi YK, Nishino I. A Gne knockout mouse expressing human GNE D176V mutation develops features similar to distal myopathy with rimmed vacuoles or hereditary inclusion body myopathy. *Hum. Mol. Genet.* 2007; 16:2669–2682. [PubMed: 17704511]
- Galeano B, Klootwijk R, Manoli I, Sun M, Ciccone C, Darvish D, Starost MF, Zervas PM, Hoffmann VJ, Hoogstraten-Miller S, Krasnewich DM, Gahl WA, Huizing M. Mutation in the key

- enzyme of sialic acid biosynthesis causes severe glomerular proteinuria and is rescued by N-acetylmannosamine. *J. Clin. Invest.* 2007; 117:1585–1594. [PubMed: 17549255]
15. Kakani S, Yardeni T, Poling J, Ciccone C, Niethamer T, Klootwijk ED, Manoli I, Darvish D, Hoogstraten-Miller S, Zerfas P, Tian E, Ten Hagen KG, Kopp JB, Gahl WA, Huizing M. The Gne M712T mouse as a model for human glomerulopathy. *Am. J. Pathol.* 2012; 180:1431–1440. [PubMed: 22322304]
  16. Malicdan MC, Noguchi S, Hayashi YK, Nonaka I, Nishino I. Prophylactic treatment with sialic acid metabolites precludes the development of the myopathic phenotype in the DMRV-hIBM mouse model. *Nat. Med.* 2009; 15:690–695. [PubMed: 19448634]
  17. Reinke SO, Lehmer G, Hinderlich S, Reutter W. Regulation and pathophysiological implications of UDP-GlcNAc 2-epimerase/ManNAc kinase (GNE) as the key enzyme of sialic acid biosynthesis. *Biol. Chem.* 2009; 390:591–599. [PubMed: 19426133]
  18. Garnier J, Osguthorpe DJ, Robson B. Analysis of the accuracy and implications of simple methods for predicting the secondary structure of globular proteins. *J. Mol. Biol.* 1978; 120:97–120. [PubMed: 642007]
  19. Kloczkowski A, Ting KL, Jernigan RL, Garnier J. Combining the GOR V algorithm with evolutionary information for protein secondary structure prediction from amino acid sequence. *Proteins.* 2002; 49:154–166. [PubMed: 12210997]
  20. Cheng H, Sen TZ, Kloczkowski A, Margaritis D, Jernigan RL. Prediction of protein secondary structure by mining structural fragment database. *Polymer. (Guildf).* 2005; 46:4314–4321. [PubMed: 19081746]
  21. Sen TZ, Cheng H, Kloczkowski A, Jernigan RL. A Consensus Data Mining secondary structure prediction by combining GOR V and Fragment Database Mining. *Protein Sci.* 2006; 15:2499–2506. [PubMed: 17001039]
  22. Bryson K, McGuffin LJ, Marsden RL, Ward JJ, Sodhi JS, Jones DT. Protein structure prediction servers at University College London. *Nucleic Acids Res.* 2005; 33:W36–38. [PubMed: 15980489]
  23. Yardeni T, Eckhaus M, Morris HD, Huizing M, Hoogstraten-Miller S. Retro-orbital injections in mice. *Lab. Anim. (NY).* 2011; 40:155–160. [PubMed: 21508954]
  24. Yardeni, T.; Ciccone, C.; Hoogstraten-Miller, S.; Darvish, D.; Anikster, Y.; Maples, PB.; Jay, CM.; Gahl, WA.; Nemunaitis, J.; Huizing, M. A Non-Viral, GNE-Lipoplex Treatment to Correct Sialylation Defects in Gne-Mutant (M712T) Mice.. *Proceedings of the American Society for Gene & Cell Therapy, Annual Meeting; Washington, DC.* 2010;
  25. Schmittgen TD, Livak KJ. Analyzing real-time PCR data by the comparative C(T) method. *Nat. Protoc.* 2008; 3:1101–1108. [PubMed: 18546601]
  26. Reinke SO, Eidenschink C, Jay CM, Hinderlich S. Biochemical characterization of human and murine isoforms of UDP-N-acetylglucosamine 2-epimerase/N-acetylmannosamine kinase (GNE). *Glycoconj. J.* 2009; 26:415–422. [PubMed: 18815882]
  27. Eisenberg I, Grabov-Nardini G, Hochner H, Korner M, Sadeh M, Bertorini T, Bushby K, Castellan C, Felice K, Mendell J, Merlini L, Shilling C, Wirguin I, Argov Z, Mitrani-Rosenbaum S. Mutations spectrum of GNE in hereditary inclusion body myopathy sparing the quadriceps. *Hum. Mutat.* 2003; 21:99. [PubMed: 12497639]
  28. Tong Y, Tempel W, Nedyalkova L, Mackenzie F, Park HW. Crystal structure of the N-acetylmannosamine kinase domain of GNE. *PLoS One.* 2009; 4:e7165. [PubMed: 19841673]
  29. Kurochkina N, Yardeni T, Huizing M. Molecular modeling of the bifunctional enzyme UDP-GlcNAc 2-epimerase/ManNAc kinase and predictions of structural effects of mutations associated with HIBM and sialuria. *Glycobiology.* 2010; 20:322–337. [PubMed: 19917666]
  30. Zhao B, Lehr R, Smallwood AM, Ho TF, Maley K, Randall T, Head MS, Koretko KK, Schnackenberg CG. Crystal structure of the kinase domain of serum and glucocorticoid-regulated kinase 1 in complex with AMP PNP. *Protein Sci.* 2007; 16:2761–2769. [PubMed: 17965184]
  31. Keppler OT, Hinderlich S, Langner J, Schwartz-Albiez R, Reutter W, Pawlita M. UDP-GlcNAc 2-epimerase: a regulator of cell surface sialylation. *Science.* 1999; 284:1372–1376. [PubMed: 10334995]

32. Krause S, Hinderlich S, Amsili S, Horstkorte R, Wiendl H, Argov Z, Mitrani-Rosenbaum S, Lochmuller H. Localization of UDP-GlcNAc 2-epimerase/ManAc kinase (GNE) in the Golgi complex and the nucleus of mammalian cells. *Exp. Cell Res.* 2005; 304:365–379. [PubMed: 15748884]
33. Ghaderi D, Strauss HM, Reinke S, Cirak S, Reutter W, Lucka L, Hinderlich S. Evidence for dynamic interplay of different oligomeric states of UDP-N-acetylglucosamine 2-epimerase/N-acetylmannosamine kinase by biophysical methods. *J. Mol. Biol.* 2007; 369:746–758. [PubMed: 17448495]
34. Yogev O, Pines O. Dual targeting of mitochondrial proteins: mechanism, regulation and function. *Biochim. Biophys. Acta.* 2011; 1808:1012–1020. [PubMed: 20637721]
35. Duncan PI, Raymond F, Fuerholz A, Sprenger N. Sialic acid utilisation and synthesis in the neonatal rat revisited. *PLoS One.* 2009; 4:e8241. [PubMed: 20011510]
36. Kontou M, Weidemann W, Bork K, Horstkorte R. Beyond glycosylation: sialic acid precursors act as signaling molecules and are involved in cellular control of differentiation of PC12 cells. *Biol. Chem.* 2009; 390:575–579. [PubMed: 19361277]
37. Kean EL, Munster-Kuhnel AK, Gerardy-Schahn R. CMP-sialic acid synthetase of the nucleus. *Biochim. Biophys. Acta.* 2004; 1673:56–65. [PubMed: 15238249]
38. Kershaw DB, Beck SG, Wharram BL, Wiggins JE, Goyal M, Thomas PE, Wiggins RC. Molecular cloning and characterization of human podocalyxin-like protein. Orthologous relationship to rabbit PCLP1 and rat podocalyxin. *J. Biol. Chem.* 1997; 272:15708–15714. [PubMed: 9188463]
39. Chou HH, Takematsu H, Diaz S, Iber J, Nickerson E, Wright KL, Muchmore EA, Nelson DL, Warren ST, Varki A. A mutation in human CMP-sialic acid hydroxylase occurred after the Homo-Pan divergence. *Proc. Natl. Acad. Sci. U S A.* 1998; 95:11751–11756. [PubMed: 9751737]
40. Nemunaitis G, Maples PB, Jay C, Gahl WA, Huizing M, Poling J, Tong AW, Phadke AP, Pappen BO, Bedell C, Templeton NS, Kuhn J, Senzer N, Nemunaitis J. Hereditary inclusion body myopathy: single patient response to GNE gene Lipoplex therapy. *J. Gene Med.* 2010; 12:403–412. [PubMed: 20440751]
41. Nemunaitis G, Jay CM, Maples PB, Gahl WA, Huizing M, Yardeni T, Tong AW, Phadke AP, Pappen BO, Bedell C, Allen H, Hernandez C, Templeton NS, Kuhn J, Senzer N, Nemunaitis J. Hereditary Inclusion Body Myopathy: Single Patient Response to Intravenous Dosing of GNE Gene Lipoplex. *Hum. Gene Ther.* 2011; 22:1331–1341. [PubMed: 21517694]

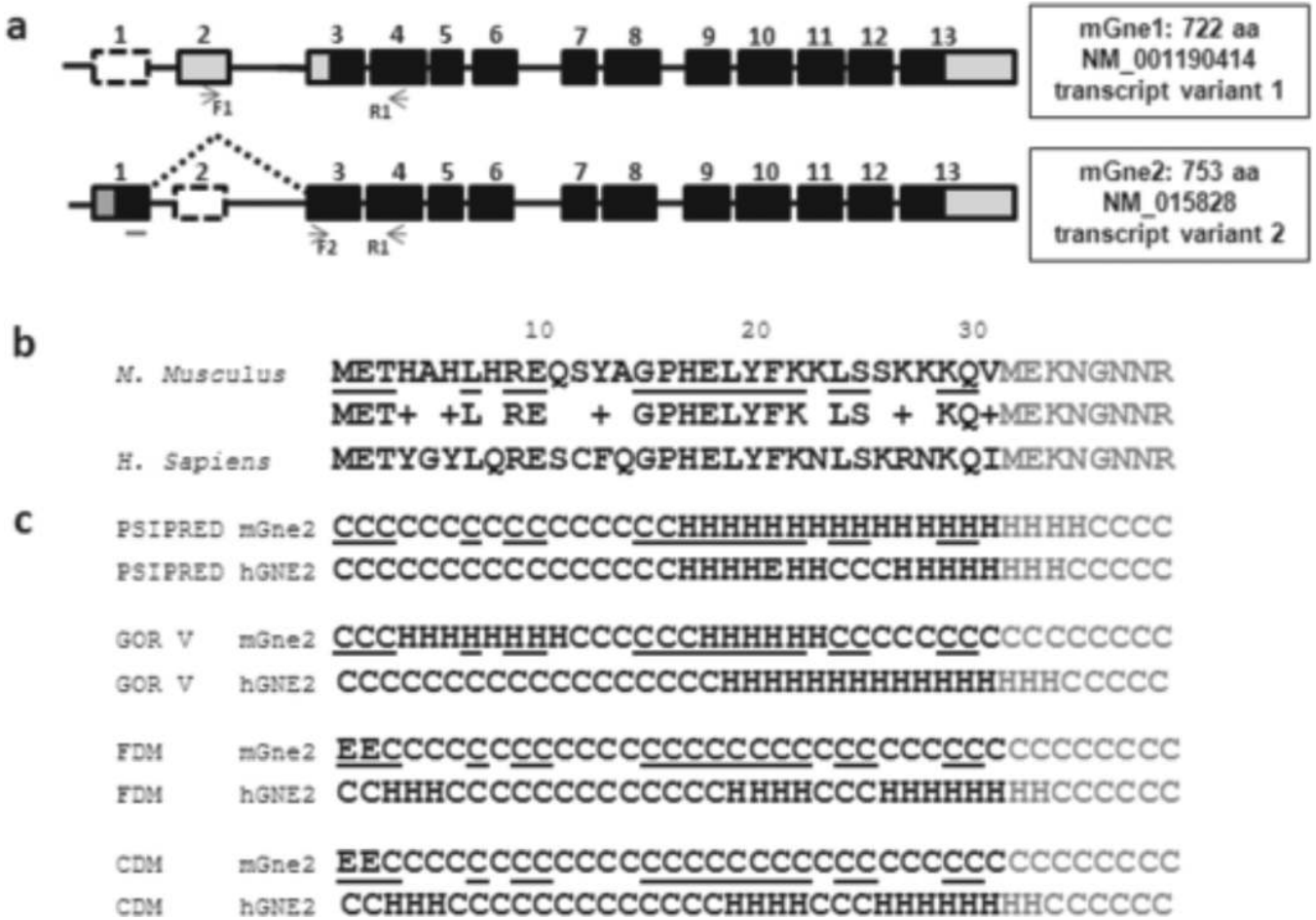
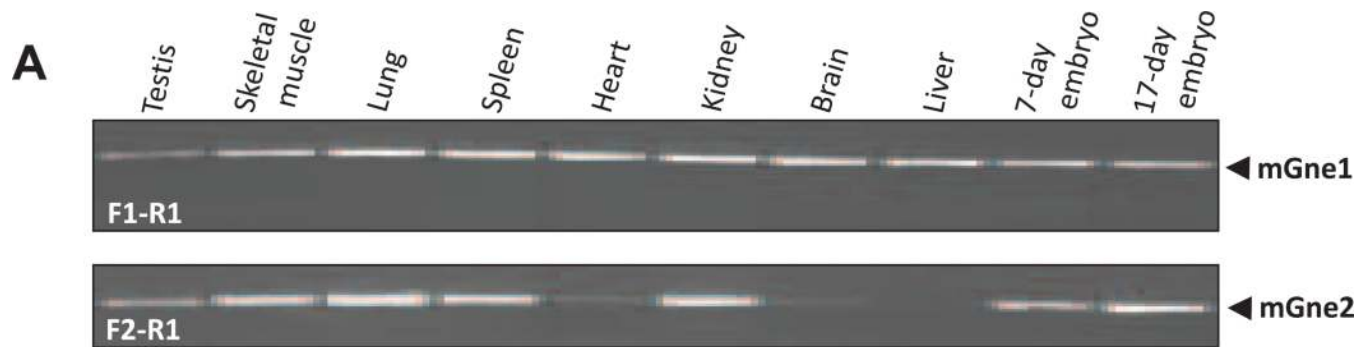


**Fig. 1. Mouse *Gne* transcripts, sequence alignment and secondary structure prediction of N-terminal extension of mGne2**

**a.** Exon (boxes)-intron (lines) structures of mouse *Gne* transcripts *mGne1* and *mGne2*. GenBank Accession numbers and predicted numbers of translated amino acids (aa) are indicated. Black boxes illustrate the open reading frame, gray boxes the untranslated mRNA regions, and dashed boxes the skipped exons of each transcript. Primer locations for transcript-specific PCR amplifications (Fig. 2) are indicated below each isoform. Note that the forward primer F2 is localized across exon1-exon3 boundaries.

**b.** Amino acid sequence alignment of the 31 residue N-terminal extensions of mouse mGne2 and human hGNE2, show only 58% identity and 74% homology. Black, 31 amino acid N-terminal extensions; Gray: overlap with mGne1 and hGNE1 amino acids; Underlined: identical amino acids in mGne2 compared to hGNE2; +: homologous amino acids.

**c.** Secondary structure predictions with 4 prediction methods (PSIPRED, GOR V, FDM, and CDM) of the N-terminal 31-residue extension mGne2 show significant differences between mGne2 and hGNE2. Black, 31 amino acid N-terminal extensions; Gray: overlap with mGne1 and hGNE1 amino acids; Underlined: identical amino acids in mGne2 compared to hGNE2; C, coil; H,  $\alpha$ -helices; E,  $\beta$ -strands.



**B**

	<i>mGne1</i>	<i>mGne2</i>	<i>hGNE1</i>	<i>hGNE2</i>
<i>Testis</i>	+	+	+	-
<i>Sk. Muscle</i>	+	+	+	-
<i>Lung</i>	+	+	+	+
<i>Spleen</i>	+	+	+	-
<i>Heart</i>	+	+	+	-
<i>Kidney</i>	+	+	+	+
<i>Brain</i>	+	+	+	-
<i>Liver</i>	+	-	+	+

**Fig. 2. Tissue-specific expression of mGne isoform transcripts**

**a.** PCR amplification of tissue-specific cDNA from selected mouse tissues. Primers and amplified transcripts are indicated.

**b.** Summary of mGne1 and mGne2 compared with hGNE1 and hGNE2 tissue-specific transcript expression.

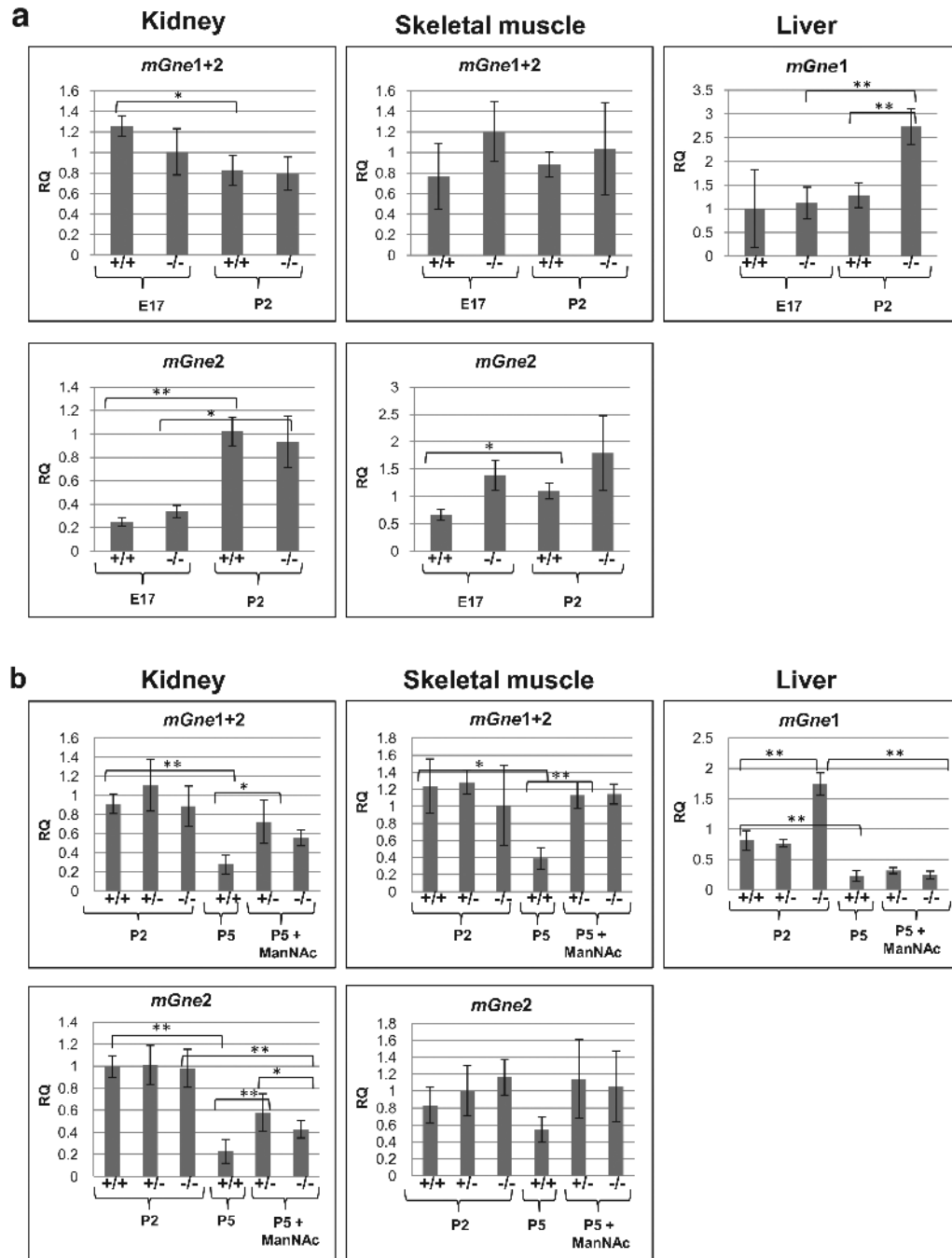


**Fig. 3. *Gne* expression in tissues of the ‘M712T knock-in’ mouse model**  
 qPCR results of isoform-specific *mGne* expression in kidney, skeletal muscle and liver tissues of the knock-in *Gne* p.M712T mouse model: +/+, wild type; +/-, heterozygous; -/-, mutant. Transcript-specific Taqman primer-probe assays were used (see Table S2), as indicated above each panel. Displayed values represent the relative quantification (RQ) normalized to *B2M* with expression in wild type (+/+) at P2 set to 1 for each Taqman probe. P-values 0.01-0.05 (\*), <0.01(\*\*) (Statistical data are displayed in Tables S3a and S3b).  
**a.** *mGne* tissue-specific transcript expression at embryonic day 17 (E17) and postnatal day 2 (P2).

**b.** mGne tissue-specific transcript expression in untreated tissues at P2 (all genotypes) and P5 (wild type only), and in tissues after ManNAc treatment at P5 (heterozygous and mutant).

**Table 1**

Amino acid similarities between the N-terminal 31 amino acid extension of mGne2 and other homologous proteins

Protein/source/pdb code/	aa # <sup>a</sup>	Sequence alignment <sup>b</sup>
mGne2 extension	1-31	METHAHLHREQSYAGPHELYFKKLSSKKKQV
hGNE2 extension	1-31	METYGYLQRESCFQGPHELYFKNLSKRNKQI
SGK1/ <i>H. sapiens</i> /2r5t/	183-202	ELFYHLQRERCFLEPRARFY
His kinase/ <i>A. avenae</i> /	198-213	FLQRERCFAGDASHEL
His kinase/ <i>P. carotovorum</i> /	194-219	DELERFLQRERCFVSDASHELRTPLA
His kinase/ <i>H. arsenicoxydans</i> /	193-216	AELQQFLARERFFTGDVSHEL RTP
Ser/Thr protein kinase/ <i>H. sapiens</i> /2vx3/	104-131	HHHHHSSGVDLGTENLYFQSMSSHKKE
DYRK2/ <i>H. sapiens</i> /3k2l/	107-122	EIYFLGLNAKKRQG
PRPP amidotransferase/ <i>B. subtilis</i> /1ao0/	18-48	YGLHSLOHRGQEGAGIVATDGEKLTAKGQG
PRPP amidotransferase / <i>E. coli</i> /1ecb/	18-48	DALTVLQHRGQDAAGIITIDANDCFRLRKAN
VAV1/ <i>H. sapiens</i> / 3bjj	465-495	KWSHMFLLIEDQGAQGYELFFKTRELKWKWM
Carbonic anhydrase IV/ <i>H. sapiens</i> /1znc/	217-247	QLHREQILAFSQKLYYDK
GCNA/ <i>S. gordonii</i> /2ep1/	51-81	SYKQPHQLY
Oxidoreductase/ <i>E. coli</i> /1tlt/	149-165	HRSNS-VGPHDLYFTLL
Deoxyribonuclease/ <i>T. maritima</i> /1j6o/	1-11	VDTHAHLHFHQ

<sup>a</sup> aa #: amino acid number

<sup>b</sup> Shaded: identical amino acids; double underlined:  $\alpha$ -helices; underlined:  $\beta$ -sheets. No secondary structure data are known about protein fragments lacking underlining